1982

Measurements of an e 1-M 1 interference effect in the electric-field quenching of spin-polarized He+2s12 ions

A. Van Wijngaarden

Gordon W. F. Drake
University of Windsor

PHYSICAL REVIEW A VOLUME 25, NUMBER 1 JANUARY 1982

Measurements of an $E1$-$M1$ interference effect in the electric-field quenching of spin-polarized He^+ $2s_{1/2}$ ions

A. van Wijngaarden and G. W. F. Drake
Department of Physics, University of Windsor, Windsor, Ontario, Canada N9B 3P4
(Received 13 May 1981)

When a beam of spin-polarized metastable He^+ $2s_{1/2}$ ions is quenched by an electric field $\vec{E}$, the emitted radiation intensity contains an asymmetry term which is proportional to $\hat{k}\cdot\vec{E}\times\vec{P}$, where $\vec{P}$ is the spin-polarization vector and $\hat{k}$ is the direction of observation. The effect is due to interference between spontaneous magnetic-dipole ($M1$) and induced electric-dipole ($E1$) decay modes to the ground state. At $|\vec{E}| = 38.14$ V/cm, the measured asymmetry is $(0.323\pm0.085)\times10^{-3}$ in agreement with the theoretical value 0.3443×10^{-3}. The experiment provides the first measurement of the relativistic $M1$ matrix element for the $2s_{1/2}$-$1s_{1/2}$ transition in a hydrogenic ion. The paper contains an extensive discussion of all possible asymmetry effects, including higher-order relativistic and electric-field perturbation corrections.

I. INTRODUCTION

There has recently been considerable interest in measuring the radiation asymmetries in atomic and molecular transitions caused by interference between electric-field-induced electric-dipole ($E1$) and magnetic-dipole ($M1$) transitions.[1-3] In analogy with the theory of molecular optical activity,[4] the electric field destroys the atomic inversion symmetry and weakens the parity selection rule. Consequently, both $E1$ amd $M1$ transitions become simultaneously allowed. Interference terms cause a number of asymmetries in the polarization and angular distribution of the emitted radiation. Some of these effects have been observed in cesium,[1] thallium,[2] and methane.[3]

It has recently been pointed out[5-7] that similar effects should be observable in the $2s_{1/2}$-$1s_{1/2}$ transition of hydrogenic ions. It is particularly important to observe the effects in this most fundamental of atomic systems since precise theoretical predictions are possible. The predicted asymmetries should be taken into account in the analysis of quench rate[8] and quenching anisotropy[9] methods of measuring the Lamb shift.

In this paper, we report the first measurement of an $E1$-$M1$ interference effect in a hydrogenic system. As proposed previously,[7] the experiment starts with a spin-polarized beam of He^+ ions in the metastable $2s_{1/2}$ state. The ions are quenched to the ground state by application of a dc electric field, and a small asymmetry is observed in the emitted Lyα radiation with respect to a mirror reflection of the total intensity through the plane containing the dc electric-field vector and the spin polarization vector. The experiment can be interpreted as the first measurement of the $2s_{1/2}$-$1s_{1/2}$ $M1$ transition matrix element in a hydrogenic system. Alternatively, it is a method of measuring the degree of spin polarization in the initial beam. This may prove to be a useful experimental technique for heavier hydrogenic ions such as Ne^{9+}.

In Sec. II of the paper, we first review the theory of quenching asymmetries in hydrogenic systems, and obtain a general expression containing all possible effects exhibited by the quenching radiation. Since the same quenching theory can be used in a number of other experiments, the presentation is more general than what is required for the present work. The experimental method is then described in Sec. III and the results are presented in Sec. IV.

II. QUENCHING THEORY

The conventional method for describing the electric-field quenching of the metastable $2s_{1/2}$ state of hydrogenlike systems is based on the phenomenological Bethe-Lamb quenching theory,[10] which is, in turn, derived from the Wigner-Weisskopf[11] analysis for time-dependent perturbations. Calculations have been done by many authors within this framework.[9,12-15] Recently, Kelsey and Macek[16] and Hillery and Mohr[6] have shown from quantum electrodynamics that the Bethe-Lamb formalism has a rigorous foundation

to lowest relative order in α/π. The key point is that it is consistent to use relativistic wave functions for the evaluation of matrix elements, together with relativistic energy denominators which contain also the Lamb shift and imaginary level widths. Hillery and Mohr also include the contributions from $M1$ and $M2$ transitions, and discuss the rotational asymmetries they produce in the quenching radiation. In this section, we use the Bethe-Lamb formalism to extend their results to a complete description of all possible rotational asymmetries and photon polarization phenomena, including higher-order perturbation corrections due to the external electric field. Since ${}_2He_4{}^+$ has zero nuclear spin, additional hyperfine-structure effects are not discussed.

A. Formulas for quenching asymmetries

In the presence of a static external field, the $2s_{1/2}$ state can decay by spontaneous $M1$ transitions to the ground state, or by electric-field-induced $E1$ and $M2$ transitions due to intermixing with the $2p_{1/2}$ and $2p_{3/2}$ states. Spontaneous $2E1$ transitions also occur, but these do not produce interference effects with the single-photon transitions, and can therefore be treated as a constant background. The Dirac transition operator for single-photon emission is

$$A^* = \vec{\alpha}\cdot\hat{e}e^{-i\vec{k}\cdot\vec{r}} , \tag{2.1}$$

where $\hat{e}$ is the photon polarization vector and $\vec{k}$ is the propagation vector ($|\vec{k}| = \omega/c$). If A^* is expanded into multipoles and only the $E1$, and $M1$, and $M2$ contributions retained, then

$$A^* = \left[\frac{3}{8\pi}\right]^{1/2} \sum_M \{ e_M \tilde{a}^{(1)*}_{1M} + i(\tfrac{10}{3})^{1/2}[\hat{k},\hat{k}\times\hat{e}]_{2,M}\tilde{a}^{(0)*}_{2M} + i[\hat{k}\times\hat{e}]_M \tilde{a}^{(0)*}_{1M} \} , \tag{2.2}$$

where the e_M denote the irreducible tensor components

$$e_{\pm1} = \mp\frac{1}{\sqrt{2}}(e_x \pm ie_y) ,$$
$$e_0 = e_z , \tag{2.3}$$

the notation $[\hat{a},\hat{b}]_{2,M}$ denotes the vector-coupled product

$$[\hat{a},\hat{b}]_{2,M} = \sum_{m_1,m_2} \langle 1,m_1,1,m_2 \mid 2,M\rangle a_{m_1} b_{m_2} , \tag{2.4}$$

and

$$\tilde{a}^{(\lambda)*}_{LM} = \vec{\alpha}\cdot\vec{a}^{(\lambda)*}_{LM} , \tag{2.5}$$

where the $\vec{a}^{\lambda*}_{LM}$ are the standard operators for electric multipole ($\lambda=1$) and magnetic multipole ($\lambda=0$) transitions as given, for example, by Akhiezer and Berestetskii.[17] In the nonrelativistic limit, the $\tilde{a}^{(\lambda)*}_{LM}$ reduce to

$$\tilde{a}^{(1)*}_{1M} \simeq \sqrt{2}\Phi^*_{1M} , \tag{2.6}$$

$$\tilde{a}^{(0)*}_{1M} \simeq -i\vec{\nabla}(\Phi^*_{1M})\cdot\left[\frac{e\vec{L}}{\sqrt{2}mc} + \sqrt{2}\vec{\mu}\right] , \tag{2.7}$$

$$\tilde{a}^{(0)*}_{2M} \simeq -i\vec{\nabla}(\Phi^*_{2M})\cdot\left[\frac{e\vec{L}}{\sqrt{6}mc} + \left[\frac{3}{2}\right]^{1/2}\vec{\mu}\right] , \tag{2.8}$$

where

$$\Phi_{LM} = 4\pi i^L j_L(kr) Y^M_L(\hat{r}) , \tag{2.9}$$

$$\vec{\mu} = \frac{e\hbar}{2mc}\vec{\sigma} , \tag{2.10}$$

$\vec{L} = \vec{r}\times\vec{p}$, and $j_L(kr)$ is a spherical Bessel function.

The first two terms of (2.2) (i.e., the $E1$ and $M2$ parts) contribute to $2s_{1/2}$-$1s_{1/2}$ transitions only through the external field mixing of s and p states. For He^+ in electric fields up to several kV/cm, the only significant mixing is among the manifold of states $2s_{1/2}$, $2p_{1/2}$, and $2p_{3/2}$. If the electric field $\vec{E}$ is switched on adiabatically, then the perturbed $2s_{1/2}$ initial state can be written in the form

$$\psi(2s_{1/2},m)=a\psi_0(2s_{1/2},m)+\sum_{m'}[b^{(1/2)}_{m,m'}\psi_0(2p_{1/2},m')+b^{(3/2)}_{m,m'}\psi_0(2p_{3/2},m')] , \tag{2.11}$$

where the matrices $\underline{b}^{(j)}$ ($j=\frac{1}{2},\frac{3}{2}$) are given by

$$\underline{b}^{(1/2)}=b_{1/2}(\vec{\sigma}\cdot\hat{E}) , \tag{2.12}$$

$$\underline{b}^{(3/2)}=b_{3/2}\begin{bmatrix}-\sqrt{3}E_{-1} & \sqrt{2}E_0 & -E_1 & 0\\ 0 & -E_{-1} & \sqrt{2}E_0 & \sqrt{3}E_1\end{bmatrix} , \tag{2.13}$$

and the E_i ($i=0,\pm1$) are the irreducible tensor components of the unit vector $\hat{E}$ in the electric-field direction. The above form remains valid to all orders of perturbation theory since the perturbation operator $e\vec{E}\cdot\vec{r}$ is an operator of odd parity which does not lift the degeneracy of the $2s_{1/2}$ ($m=\pm\frac{1}{2}$) state. To lowest order, the a and b_j are given by (in atomic units)

$$a=1+O(|\vec{E}|^2) , \tag{2.14}$$

$$b_{1/2}=\frac{|\vec{E}|\langle 2p_{1/2}||\vec{r}||2s_{1/2}\rangle}{\sqrt{6}[E(2s_{1/2})-E(2p_{1/2})+i\Gamma/2]}+O(|\vec{E}|^3) , \tag{2.15}$$

$$b_{3/2}=\frac{|\vec{E}|\langle 2p_{3/2}||\vec{r}||2s_{1/2}\rangle}{\sqrt{12}[E(2s_{1/2})-E(2p_{3/2})+i\Gamma/2]}+O(|\vec{E}|^3) , \tag{2.16}$$

where Γ is the lifetime of the $2p$ state, and the reduced matrix element notation of Edmonds[18] has been used. Higher-order perturbation corrections are discussed below. The a and b_j could also be calculated by an exact diagonalization of the Hamiltonian matrix in the $2s_{1/2}$, $2p_{1/2}$, $2p_{3/2}$ basis set.

The properties of the quenching radiation are determined by the matrix elements

$$A_{m,m'}=\langle 1s_{1/2},m\,|A^*|\,2s_{1/2},m'\rangle \tag{2.17}$$

between the unperturbed $1s_{1/2}$ final state and the perturbed $2s_{1/2}$ initial state as given by (2.11). The matrix elements of the $\tilde{a}^{(\lambda)*}_{LM}$ can be expressed in terms of reduced matrix elements by means of the Wigner-Eckart theorem. After some further algebra, it can be shown that the 2×2 transition matrix $\underline{A}$ with elements $A_{m,m'}$ is given by

$$\underline{A}=V_+\hat{e}\cdot\hat{E}\underline{1}+\vec{\sigma}\cdot[iV_-(\hat{e}\times\hat{E})+M(\hat{k}\times\hat{e})] , \tag{2.18}$$

where

$$\begin{aligned}V_+&=V_{1/2}+2V_{3/2} ,\\ V_-&=V_{1/2}-V_{3/2}+M_{3/2} ,\\ M&=M_{1/2}+2i(\hat{k}\cdot\hat{E})M_{3/2} ,\end{aligned} \tag{2.19}$$

and

$$\begin{aligned}V_{1/2}&=\frac{-b_{1/2}}{4\pi^{1/2}}\langle 1s_{1/2}||\tilde{a}^{(1)*}_1||2p_{1/2}\rangle ,\\ V_{3/2}&=\frac{-b_{3/2}}{4(2\pi)^{1/2}}\langle 1s_{1/2}||\tilde{a}^{(1)*}_1||2p_{3/2}\rangle ,\\ M_{1/2}&=\frac{ia}{4\pi^{1/2}}\langle 1s_{1/2}||\tilde{a}^{(0)*}_1||2s_{1/2}\rangle ,\\ M_{3/2}&=\frac{-b_{3/2}}{4(2\pi/3)^{1/2}}\langle 1s_{1/2}||\tilde{a}^{(0)*}_2||2p_{3/2}\rangle .\end{aligned} \tag{2.20}$$

Numerical values for the quantities in (2.20) are given in Sec. II C.

In addition to the $\hat{e}$ and $\vec{k}$ vectors describing the polarization and direction of emission of the photon, the quenching radiation also depends on the electron-spin polarization of the initial $2s_{1/2}$ state. This is specified, in general, by the density matrix

$$\underline{\rho}=\tfrac{1}{2}(\underline{1}+\vec{\sigma}\cdot\vec{P}) , \tag{2.21}$$

where $\vec{P}$ is the polarization vector. The decay rate per unit solid angle is then

$$I(\hat{e},\vec{k},\vec{P})=\frac{\alpha k}{4\pi}\mathrm{Tr}[\underline{\rho}\underline{A}^{\dagger}\underline{A}] . \tag{2.22}$$

For convenience in expressing the final results, we choose a coordinate system such that $\hat{k}$ lies along

the z axis, and $\hat{e}$ for the general case of elliptical polarization is given by

$$\hat{e}=\cos\beta\hat{i}+i\sin\beta\hat{j} . \tag{2.23}$$

We also introduce an auxiliary vector $\vec{E}'$ defined by

$$\vec{E}'=E_x\hat{i}-E_y\hat{j} , \tag{2.24}$$

where E_x and E_y are the x and y components of the unit vector $\hat{E}$ in the field direction. Then, using (2.18) and (2.21), Eq. (2.22) can be written in the form

$$I(\hat{e},\hat{k},\vec{P})=\frac{\alpha k}{4\pi}[I_0+\vec{P}\cdot\vec{J}_0+\vec{P}\cdot\vec{J}_1\sin2\beta + \vec{E}'\cdot\vec{J}_2\cos2\beta] , \tag{2.25}$$

where

$$I_0=\tfrac{1}{2}|V_+|^2[1-(\hat{k}\cdot\hat{E})^2]+\tfrac{1}{2}|V_-|^2[1+(\hat{k}\cdot\hat{E})^2] + |M|^2-2\,\mathrm{Im}(M^*V_-)(\hat{k}\cdot\hat{E}) , \tag{2.26}$$

$$\vec{J}_0=(\hat{k}\times\hat{E})\{\mathrm{Re}[M^*(V_++V_-)] -\mathrm{Im}(V_-^*V_+)(\hat{k}\cdot\hat{E})\} , \tag{2.27}$$

$$\vec{J}_1=|V_-|^2(\hat{k}\cdot\hat{E})\hat{E} +\mathrm{Re}(V_-^*V_+)\hat{E}(\hat{k}\times\hat{E}) -|M|^2\hat{k}-\mathrm{Im}[M^*(V_++V_-)]\hat{E} -\mathrm{Im}[M^*(V_+-V_-)](\hat{k}\cdot\hat{E})\hat{k} , \tag{2.28}$$

and

$$\vec{J}_2=\tfrac{1}{2}(|V_+|^2-|V_-|^2)\hat{E}+\mathrm{Im}(V_-^*V_+)\hat{E}\times\vec{P} +\mathrm{Re}[M^*(V_++V_-)]\vec{P}\times\hat{k} . \tag{2.29}$$

The above expressions can be further expanded in terms of the V_j's and M_j's by use of (2.19). The $\sin2\beta$ and $\cos2\beta$ terms in (2.25) vanish on summing over photon polarizations, but can be observed with a polarization-sensitive detector. It is clear that the quenching radiation has a strong circular polarization proportional to $\vec{P}$ if the ion beam is initially polarized. The effect is most pronounced if $\hat{k}$ is parallel to $\vec{P}$. The linear polarization term $\vec{E}'\cdot\vec{J}_2$, which to a first approximation is independent of $\vec{P}$, has been measured by Ott, Kauppila, and Fite.[19] The present experiment is designed to measure the $\vec{P}\cdot\vec{J}_0$ term with $\hat{k}\cdot\hat{E}=0$. The only nonvanishing contribution comes from the cross term $\mathrm{Re}[M^*(V_++V_-)]$ in $\vec{J}_0$, which is the $E1$-$M1$ asymmetry.

B. Higher-field perturbation corrections

To lowest nonvanishing order in the electric-field strength, the coefficients a, $b_{1/2}$, and $b_{3/2}$ in (2.11) to (2.13) are given by (2.14)–(2.16). We calculate here higher-perturbation corrections on the assumption that only the mixing of the $2s_{1/2}$ state with $2p_{1/2}$ and $2p_{3/2}$ need by taken into account.

Since the external electric field does not lift the degeneracy of the $2s_{1/2}$ ($m=\pm\frac{1}{2}$) state, the higher-order corrections to a, $b_{1/2}$, and $b_{3/2}$ do not depend on the field direction. We therefore assume without loss of generality that the field acts in the z direction and write the perturbation operator in the form $e\mathscr{E}z$, with $\mathscr{E}=|\vec{E}|$. The $2s_{1/2}$ eigenvalue and wave function can then be expanded in the form

$$E=E_0+E_2\mathscr{E}^2+E_4\mathscr{E}^4+\cdots , \tag{2.30}$$

$$\psi=\psi_0+\psi_1\mathscr{E}+\psi_3\mathscr{E}^3+\cdots , \tag{2.31}$$

where

$$(H_0-E_0)\psi_0=0 \tag{2.32}$$

is the zero-order eigenvalue problem and the perturbation equations are (in atomic units)

$$(H_0-E_0)\psi_m+z\psi_{m-1}=\sum_{n=0}^{m}E_{m-n}\psi_n , \tag{2.33}$$

with $\psi_m=0$ for m even ($m>0$) and $E_m=0$ for m odd. Using the definitions

$$|S_l\rangle=\sum_{j=1/2}^{3/2}\frac{\langle 2s_{1/2}|z|2p_j\rangle|2p_j\rangle}{[E_0(2s_{1/2})-E_0(2p_j)+i\Gamma/2]^l} , \tag{2.34}$$

$$T_l=\sum_{j=1/2}^{3/2}\frac{|\langle 2s_{1/2}|z|2p_j\rangle|^2}{[E_0(2s_{1/2})-E_0(2p_j)+i\Gamma/2]^l} , \tag{2.35}$$

then the solutions to the perturbation equations in the $2s_{1/2}$, $2p_{1/2}$, $2p_{3/2}$ basis set can be written in the form

$$|\psi_{2m+1}\rangle=\sum_{l=0}^{m}c_{m,l}|S_{l+1}\rangle , \tag{2.36}$$

$$E_{2m+2}=\langle\psi_0|z|\psi_{2m+1}\rangle =\sum_{l=0}^{m}c_{m,l}T_{l+1} . \tag{2.37}$$

The coefficients $c_{m,l}$ are determined recursively from the equation

$$c_{m,l}=-\sum_{n=l}^{m}c_{n-1,l-1}E_{2(m-n+1)} , \tag{2.38}$$

starting with $c_{0,0}=1$ and $c_{m,l}=0$ for l negative. The above follows by substituting (2.36) into (2.33), using the identity

$$(H_0-E_0)^{-1}\,|S_l\rangle=-\,|S_{l+1}\rangle\ , \tag{2.39}$$

and equating coefficients of $|S_l\rangle$. Explicitly, the terms through fifth order are

$$|\psi_1\rangle=|S_1\rangle\ ,$$
$$|\psi_3\rangle=-E_2\,|S_2\rangle\ ,$$
$$|\psi_5\rangle=-E_4\,|S_2\rangle+E_2^2\,|S_3\rangle\ ,$$
$$E_2=T_1,\quad E_4=-T_1T_2\ .$$

The perturbed wave function (2.31), renormalized so that $\langle\psi\,|\,\psi\rangle=1$ up to fifth order, is then

$$|\psi\rangle=(1+\mathscr{E}^2U_2+\mathscr{E}^4U_4)\,|2s_{1/2}\rangle + \mathscr{E}\sum_j(1+\mathscr{E}^2W_2^{(j)}+\mathscr{E}^4W_4^{(j)})\frac{z_j}{\Delta_j}\,|2p_j\rangle\ , \tag{2.40}$$

where

$$z_j=\langle 2s_{1/2}\,|\,z\,|\,2p_j\rangle\ ,$$
$$\Delta_j=E(2s_{1/2})-E(2p_j)+i\Gamma/2\ ,$$
$$U_2=-\tfrac{1}{2}A_2\ ,$$
$$U_4=\tfrac{3}{8}A_4-A_2^2\ ,$$
$$W_2^{(j)}=-\frac{E_2}{\Delta_j}-\tfrac{1}{2}A_2\ ,$$
$$W_4^{(j)}=\frac{E_2^2}{\Delta_j^2}-\frac{E_4}{\Delta_j}+\frac{3}{8}A_4-A_2^2+\frac{A_2E_2}{2\Delta_j}\ ,$$
$$A_2=\sum_j\frac{|z_j|^2}{|\Delta_j|^2}\ ,$$
$$A_4=-2\ \mathrm{Re}(E_2/\Delta_j)A_2\ .$$

The A_2 and A_4 terms come from the renormalization of ψ. It follows immediately that the perturbation expansions of the coefficients a, $b_{1/2}$, and $b_{3/2}$ are

$$a=1+\mathscr{E}^2U_2+\mathscr{E}^4U_4+\cdots\ , \tag{2.41}$$
$$b_j=b_j^{(1)}(1+\mathscr{E}^2W_2^{(j)}+\mathscr{E}^4W_4^{(j)}+\cdots)\ , \tag{2.42}$$

where the $b_j^{(1)}$ are the first-order values given by (2.15) and (2.16).

C. Numerical values

The leading relativistic corrections to the reduced matrix elements appearing in (2.15), (2.16), and (2.20) have been calculated by Hillery and Mohr[6] and by Drake *et al.*[9] The results are

$$\langle 2p_{1/2}||\vec{r}||2s_{1/2}\rangle=\frac{3\sqrt{2}}{Z}[1-\tfrac{5}{12}\alpha^2Z^2]\ ,$$
$$\langle 2p_{3/2}||\vec{r}||2s_{1/2}\rangle=-\frac{6}{Z}[1-\tfrac{1}{6}\alpha^2Z^2]\ ,$$
$$\langle 1s_{1/2}||\vec{a}_1^{(1)*}||2p_{1/2}\rangle=\frac{i\omega\alpha}{Z}\left[\frac{2\pi}{3}\right]^{1/2}\frac{2^9}{3^5}[1-(\tfrac{11}{96}+\tfrac{3}{2}\ln 2-\ln 3)\alpha^2Z^2]\ ,$$
$$\langle 1s_{1/2}||\vec{a}_1^{(1)*}||2p_{3/2}\rangle=\frac{i\omega\alpha}{Z}\left[\frac{4\pi}{3}\right]^{1/2}\frac{2^9}{3^5}[1-(\tfrac{11}{48}+\tfrac{5}{4}\ln 2-\tfrac{3}{4}\ln 3)\alpha^2Z^2]\ ,$$
$$\langle 1s_{1/2}||\vec{a}_1^{(0)*}||2s_{1/2}\rangle=\omega Z^2\alpha^4(2\pi)^{1/2}\frac{2^4}{3^4}[1+0.4193\alpha^2Z^2]\ ,$$
$$\langle 1s_{1/2}||\vec{a}_2^{(0)*}||2p_{3/2}\rangle=\frac{i\omega^2\alpha^3}{Z}\pi^{1/2}\frac{2^8}{3^5}[1-0.1821\alpha^2Z^2]\ ,$$

where ω is the $2s_{1/2}-1s_{1/2}$ transition frequency. The relativistic corrections in the last two equations are from the numerical integrations of Hillery and Mohr. The matrix elements in (2.40) for the finite field corrections are

$$\langle 2s_{1/2}\,|\,z\,|\,2p_{1/2}\rangle=\sqrt{3}(1-\tfrac{5}{12}\alpha^2Z^2)\ ,$$
$$\langle 2s_{1/2}\,|\,z\,|\,2p_{3/2}\rangle=-\sqrt{6}(1-\tfrac{1}{6}\alpha^2Z^2)\ .$$

The coefficients U_n and $W_n^{(j)}$ depend on the values of the Lamb shift and fine-structure splitting for a particular ion. Using the input data in Table I, the values for He^+ are

$$U_2=-3.1371\times10^{-3}\ ,$$

$$U_4=-3.9365\times10^{-5}\ ,$$

$$W_2^{(1/2)}=-8.2033\times10^{-3}+0.6428\times10^{-3}i\ ,$$

$$W_4^{(1/2)}=1.7025\times10^{-5}-1.4054\times10^{-5}i\ ,$$

$$W_2^{(3/2)}=-2.6934\times10^{-3}-0.0287\times10^{-3}i\ ,$$

$$W_4^{(3/2)}=-4.1915\times10^{-5}+0.0463\times10^{-5}i\ ,$$

assuming that $\mathscr{E}$ is expressed in kV/cm. Combining the above results, the V and M terms defined by (2.20) are

$$V_{1/2}=\frac{K\mathscr{E}}{\mathscr{E}_0\Delta_{1/2}}[1-(\tfrac{51}{96}+\tfrac{3}{2}\ln2-\ln3)\alpha^2Z^2+\mathscr{E}^2W_2^{(1/2)}+\mathscr{E}^2W_4^{(1/2)}]\ , \tag{2.43}$$

$$V_{3/2}=\frac{K\mathscr{E}}{\mathscr{E}_0\Delta_{3/2}}[1-(\tfrac{19}{48}+\tfrac{5}{4}\ln2-\tfrac{3}{4}\ln3)\alpha^2Z^2+\mathscr{E}^2W_2^{(3/2)}+\mathscr{E}^4W_4^{(3/2)}]\ , \tag{2.44}$$

$$M_{1/2}=\tfrac{3}{32}KZ^4\alpha^3[1+0.4193\alpha^2Z^2+\mathscr{E}^2U_2+\mathscr{E}^4U_4]\ , \tag{2.45}$$

$$M_{3/2}=\frac{-3K\alpha^2\omega\mathscr{E}}{4\mathscr{E}_0\Delta_{3/2}}[1-0.3488\alpha^2Z^2+\mathscr{E}^2W_2^{(3/2)}+\mathscr{E}^4W_4^{(3/2)}]\ , \tag{2.46}$$

where $K=(i\omega\alpha/Z^2)(2^8/3^5\sqrt{2})$, and $\mathscr{E}_0=5.142\,25\times10^6$ kV/cm is the atomic unit of field strength. With these numerical values, all of the terms in (2.25) can be evaluated.

In the limit of small Z and weak fields, the above quantities reduce to

$$V_{1/2}\simeq\frac{(-i\omega\alpha)\mathscr{E}}{3\mathscr{E}_0\Delta_{1/2}}\langle 1s\,|\,z\,|\,2p\rangle\langle 2p\,|\,z\,|\,2s\rangle\ , \tag{2.47}$$

$$V_{3/2}\simeq\frac{(-i\omega\alpha)\mathscr{E}}{3\mathscr{E}_0\Delta_{3/2}}\langle\,|\,1s\,|\,z\,|\,2p\rangle\langle 2p\,|\,z\,|\,2s\rangle\ , \tag{2.48}$$

$$M_{1/2}\simeq(-i\omega\alpha)\langle 1s_{1/2,1/2}\,|\,M_{1,0}\,|\,2s_{1/2,1/2}\rangle\ , \tag{2.49}$$

$$M_{3/2}\simeq\frac{-3\omega\alpha^2}{4}V_{3/2}\ , \tag{2.50}$$

with

TABLE I. Input data for the calculation of the He^+ $E1$-$M1$ ions.

Quenching asymmetry	Value
$E(2s_{1/2})$-$E(2p_{1/2})$	14 042.05 MHz
$E(2p_{3/2})$-$E(2p_{1/2})$	175 594.0 MHz
$\Gamma(2p)$	1.002×10^{10} sec^{-1}
Field strength	38.14 V/cm

$$\langle 1s\,|\,z\,|\,2p\rangle=\frac{2^8}{3^5\sqrt{2}Z} \tag{2.51}$$

and

$$\langle 2p\,|\,z\,|\,2s\rangle=-3/Z\ . \tag{2.52}$$

$M_{1,0}$ in (2.49) is the z component of the magnetic-dipole moment operator, including relativistic corrections, given by[20]

$$M_{1,0}=\mu_z\left[1-\frac{2p^2}{3mc^2}-\frac{1}{6}\left[\frac{\omega r}{c}\right]^2+\frac{Ze^2}{3mc^2r}\right]\ , \tag{2.53}$$

and thus

$$\langle 1s_{1/2,1/2}\,|\,M_{1,0}\,|\,2s_{1/2,1/2}\rangle=-\frac{8\alpha^2Z^2}{81\sqrt{2}}\frac{e\hbar}{mc}\ . \tag{2.54}$$

III. EXPERIMENTAL

A. Beam preparation

The geometry of the experiment is evident from Fig. 1 of the apparatus. A beam of He^+ $2s_{1/2}$ ions polarized in the y direction is quenched by an elec-

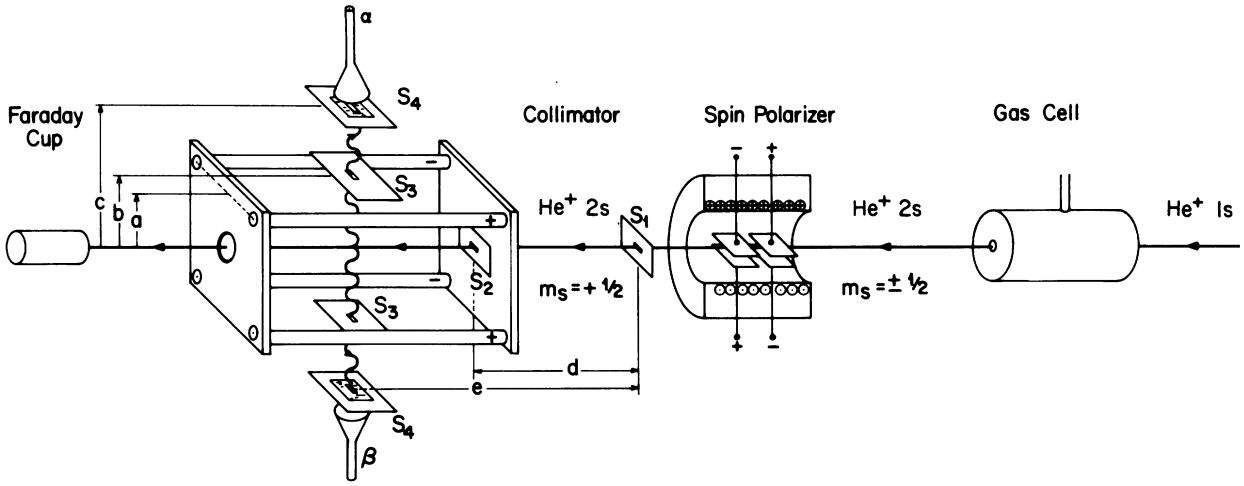

FIG. 1. Diagram of the apparatus. The dimensions shown are $a=1.616$ cm, $b=6.0$ cm, $c=22$ cm, $d=50$ cm, and $e=56$ cm. The slits S_1 and S_2 are 0.030 cm$\times$0.15 cm and the slits S_3 and S_4 are 1.0 cm$\times$0.80 cm.

tric field in the x direction and the quenching radiation intensities compared in the $+z$ and $-z$ directions with polarization-insensitive channeltron detectors. The beam of polarized $2s_{1/2}$ ions is prepared as follows. A beam of ground state $He^+1s_{1/2}$ ions with a kinetic energy of 100 keV obtained from a magnetic analyzer is passed through a gas cell for electronic excitation as shown in Fig. 1. The emerging beam contains a substantial fraction of ions in the $2s_{1/2}$ state with equal populations in the $m_j=\pm\frac{1}{2}$ magnetic substates. Ground-state ions and neutral atoms formed by charge exhange are also present, but these make no contribution to the quenching signal in the observation region. Other excited states have sufficient time to decay before reaching the observation region.

Next, the beam enters a spin polarizer consisting of an axial magnetic field of 6500 G produced by a solenoid, and a static electric field of 400 V/cm which is perpendicular to the magnetic field and produced by two pairs of parallel plates. The electric field acts over an effective distance of 5 cm along the beam axis. Using two pairs of plates with reversed polarities ensures that the beam emerges parallel to the magnetic field with no net angular deflection. In the magnetic field region, the magnetic sublevels are Zeeman split as shown in Fig. 2. As is well known, the selection rule $\Delta m_j=\pm1$ on the electric-field perturbation strongly couples the close-lying states $2s_{1/2,-1/2}$ and $2p_{1/2,1/2}$, causing $2s_{1/2,-1/2}$ to decay much more rapidly than $2s_{1/2,1/2}$. The quench rate $\gamma_{\pm1/2}$ of the $2s_{1/2,\pm1/2}$ state is approximately (see, e.g., Kugel *et al*[21]).

$$\gamma_{\pm1/2}\simeq\Gamma\frac{3e^2(a_0/Z)^2\mathscr{E}^2}{\hbar^2[(\mathscr{L}\pm\frac{4}{3}\mu_B B)^2+\Gamma^2/4]},$$

where a_0 is the Bohr radius, μ_B is the Bohr magneton, $\mathscr{L}$ is the Lamb shift, and B is the magnetic

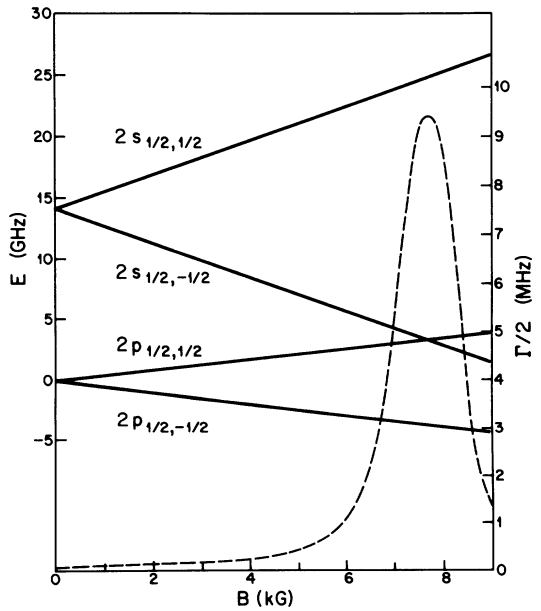

FIG. 2. Graph of the $2s_{1/2}$ and $2p_{1/2}$ magnetic sublevel energies (left-hand scale) as a function of the magnetic field strength. The dashed curve shows the $2s_{1/2,-1/2}$ level half-width (right-hand scale) for an electric quenching field strength of $\mathscr{E}=100$ V/cm.

field strength. For He^+ and $B=6500$ G, $\gamma_{-1/2} \simeq 150\gamma_{1/2}$. With $\mathscr{E}=400$ V/cm, virtually all the $2s_{1/2,-1/2}$ ions are qenched, while most of the $2s_{1/2,1/2}$ ions survive. The spin-polarization vector $\vec{P}$ is either parallel or antiparallel to the beam velocity, depending on the magnetic field direction and $|\vec{P}| \simeq 1$. After collimation by rectangular slits S_1 and S_2, the beam enters the observation region.

B. The quenching cell and photon counting

The quenching cell is the same as that described previously.[9] It contains four metal rods mounted on insulators in a quadrupole arrangement. Static voltage are applied to the rods to produce a transverse quenching field at the beam. The Lyα radiation is observed simultaneously in two opposite directions perpendicular to the field and the beam axis, with a double-photon counting system. Counting times are normalized by monitoring the beam with a Faraday cup. The cup current is 5 μA and contains a few percent of metastable He^+ $(2s, m_s=+\frac{1}{2})$ ions.

Some of the electrons and low-energy atomic particles that are formed by the interaction of the fast ion beam with the residual gas in the observation region travel, together with the Lyα radiation, into the solid angle of the photon channeltron detectors. To prevent particles from being counted, the openings of slits S_4 are covered with thin aluminum foils of a few hundred angstrom thickness. The foils are almost completely transparent to the 300-Å Lyα radiation but are thick enough to stop low-energy particles. This technique reduces the background noise by an order of magnitude.

The determination of the asymmetry $A=(I^+ - I^-)/(I^+ + I^-)$ does not require the measurement of absolute intensities. Since A can be written as $A=(r-1)/(r+1)$, where $r=I^+/I^-$, only the ratio between the intensities need be measured. The ratio independent of the detector efficiencies can be obtained from the following two measurements. First, with the electric-field direction out of the page and $\vec{P}$ parallel to the beam, the α counter monitors I^+, which views the radiation in the positive $\hat{x}$ $(\hat{x}=\hat{P}\times\hat{E})$ direction. Its signal output S_α is given by $S_\alpha=\alpha I^+$, where the constant α contains the solid angle and the (unknown) efficiency for photon detection. Similarly, the signal output of the β counter is $S_\beta=\beta I^-$. The observed signal ratio in this first experiment is

$$(S_\alpha/S_\beta)_1=(\alpha/\beta)I^+/I^- .$$

Next the electric field is reversed, leaving the detectors in a fixed position, thereby reversing the roles of the photon counters. The newly observed signal ratio now becomes

$$(S_\beta/S_\alpha)_2=(\beta/\alpha)I^+/I^- .$$

Combining the signal ratios yields

$$I^+/I^-=[(S_\alpha/S_\beta)_1(S_\beta/S_\alpha)_2]^{1/2} .$$

Thus the efficiencies of the detectors do not have to be known, and beam intensity fluctuations alone do not affect I^+/I^-.

The ratio thus found was corrected for noise, defined as the signal counts still observed with the electric field switched off. At our low quenching field of 38.14 V/cm, the noise counts were 25% of the signal counts.

C. Instrumental asymmetry

Since the $E1$-$M1$ asymmetry being measured is small, instrumental asymmetries arising from small beam displacements from the central axis must be minimized by strong collimation. For the collimator shown in Fig. 2 the instrumental asymmetry can fluctuate between zero and $A_{\text{inst}}=\pm 0.0015$. It vanishes for maximum current into the Faraday cup, indicating that the incident beam axis coincides with that of the collimator. It has its maximum value when the cup current vanishes, since then slit S_2 cuts off most of the incident beam and what remains has it maximum transverse displacement in the direction of one of the photon counters.

Since the beam current entering the collimator was very stable, small changes in beam direction leaving the collimator revealed themselves by large fluctuations in the Faraday cup current. Data were only taken when this current remained stable. For current fluctuations of 10% or more, the instrumental asymmetry is of the same order than that for the $E1$-$M1$ interference and the corresponding data were discarded. Errors that still arise from smaller random changes in beam direction are also random and do not introduce a net shift in the measured $E1$-$M1$ asymmetry.

IV. EXPERIMENTAL RESULTS

The $E1$-$M1$ asymmetry was measured as described in the previous section using 26 separate

runs made on different days. The same quenching field strength of $\mathscr{E}=38.14$ V/cm was used in all the runs. The direction of the spin polarization was reversed in five of the runs to verify that the sign of A reverses as it should. The results are shown in Table II. Each run consists of a large number of separate measurements of A as given by the column labeled N. Each measurement contains about 80 000 photon counts, of which half were taken with the electric-field direction reversed to eliminate the dependence of the results on the relative sensitivities of the photon counters (see Sec. III B). The frequent reversal of field direction also minimizes systematic errors caused by slow drifts in relative detector efficiency. At our average count rate of 800 per sec each measurement takes about 2 min. All measurements were retained in computing the averages for each run, except for runs 16, 17, 20, and $4R$. These clearly contained anomalous measurements, which were removed by discarding values lying more than two standard deviations from the mean. The mean and statistical error shown in Table II for each run were computed from

$$\bar{A}=\sum_{i=1}^{N}\frac{A_i n_i}{n_T} \tag{4.1}$$

and

$$\sigma=\left[\sum_{i=1}^{N}\frac{(A_i-\bar{A})^2 n_i}{n_T(N-1)}\right]^{1/2}, \tag{4.2}$$

where n_i is the number of counts in the ith measurements and n_T is the total number of counts for the run.

Averages over the runs were computed with a weighting factor of $1/\sigma_i^2$, where σ_i is the statistical uncertainty for the ith run. The average for runs $1-21$ is

$$\bar{A}=(0.322\pm0.097)\times10^{-3}$$

and the average for runs $1R-5R$ with $\vec{\mathrm{P}}$ reversed is

$$\bar{A}=-(0.325\pm0.16)\times10^{-3}\ .$$

TABLE II. Experimental results for $\bar{A}$. N is the number of measurements and n_T is the total number of photon counts recorded for each run.

Run	N	$n_T\times10^{-7}$	$\bar{A}\times10^{3}$
1	255	3.57	0.116±0.432
2	112	0.88	0.107±0.491
3	77	0.60	0.681±0.631
4	200	1.67	0.414±0.333
5	132	1.06	0.207±0.427
6	86	0.67	0.251±0.442
7	123	1.03	−0.106±0.637
8	85	0.95	0.281±0.742
9	130	1.01	0.604±0.512
10	100	0.74	0.524±0.477
11	160	1.18	0.570±0.404
12	198	1.45	0.395±0.364
12	160	1.21	0.080±0.460
14	121	0.87	−0.126±0.602
15	65	0.51	0.251±0.558
16	170	1.21	0.052±0.503
17	90	0.63	0.647±0.473
18	100	0.71	0.383±0.416
19	50	0.35	0.373±0.609
20	107	0.77	0.428±0.445
21	50	0.35	0.173±0.571
$1R$	100	0.78	−0.365±0.446
$2R$	210	1.64	−0.192±0.278
$3R$	175	1.28	−0.438±0.327
$4R$	130	0.92	−0.308±0.374
$5R$	300	2.14	−0.438±0.436

The two values are in good agreement. Taking all the data together (and reversing the sign for runs $1R-5R$), the final average is

$$\bar{A}=(0.323\pm0.085)\times10^{-3}\ .$$

Systematic errors resulting from stray fields in the quenching cell or instrumental asymmetries were carefully searched for, and kept small compared to the statistical uncertainty in the results.

With $|\vec{P}|=1$, $\vec{P}\cdot\hat{k}\times\hat{E}=1$, and $\hat{k}\cdot\hat{E}=0$, the theoretical value of the asymmetry for polarization-insensitive detectors is [see Eq. (2.25)]

$$A=2\ \mathrm{Re}[M^*_{1/2}(2V_{1/2}+V_{3/2}+M_{3/2})]/I_0\ , \quad (4.3)$$

where $I_0=|V_+|^2+|V_-|^2+2|M|^2$. The $M_{3/2}$ term in the numerator of (4.3), the $|M|^2$ term in I_0, and the relativistic corrections all change A by less than 0.01%, and thus may be neglected to the accuracy of the present experiment. To lowest order in the field strength, A then reduces to

$$A=\frac{6\ \mathrm{Re}(\Delta_{1/2})\langle 1s_{1/2,1/2}|M_{0,1}|2s_{1/2,1/2}\rangle}{e^2\mathscr{E}\langle 1s|z|2p\rangle\langle 2p|z|2s\rangle}\times\left[\frac{1+\frac{1}{2}|\rho|^2\mathrm{Re}(\Delta_{3/2})/\mathrm{Re}(\Delta_{1/2})}{1+\mathrm{Re}(\rho)+5|\rho|^2/2}\right], \quad (4.4)$$

where $\rho=\Delta_{1/2}/\Delta_{3/2}$. Using the numerical values in Table I and Sec. II C, the factor in square brackets is 1.026 12 and the numerical value of A is $0.013\,13/\mathscr{E}$ with $\mathscr{E}$ in V/cm. At our field strength $\mathscr{E}=38.14$ V/cm, this yields $A=0.3443\times10^{-3}$, in good agreement with the experimental value $(0.323\pm0.085)\times10^{-3}$. If the experiment is regarded as a measurement of the relativistic magnetic dipole matrix element, then

$$\langle 1s_{1/2,1/2}|M_{0,1}|2s_{1/2,1/2}\rangle=-(0.262\pm0.069)\frac{\alpha^2e\hbar}{mc}\ ,$$

in agreement with the theoretical value $-0.2794\alpha^2e\hbar/(mc)$ obtained from (2.54). No other measurements of the above matrix element in hydrogenic ions have been made.

Except for the influence of background effects, the counting time required to achieve a given relative precision in A is independent of $\mathscr{E}$, since $A\propto1/\mathscr{E}$ and $\Delta A\propto1/(\mathscr{E}t^{1/2})$. The choice $\mathscr{E}=38.14$ V/cm represents a balance between having an adequate signal-to-noise ratio, and not making A too small.

V. DISCUSSION

The apparatus and methods used in the present work are very similar to those used previously in our anisotropy measurement of the Lamb shift of He^+.[9] There, the intensities $I_{||}$ and $I_\perp$ emitted in directions parallel and perpendicular to the quenching field direction are measured simultaneously. Since the present asymmetry is quite small (~350 ppm), the good agreement between theory and experiment provides a significant check of the techniques used in the Lamb shift measurement. Since the Lamb shift experiment is substantially simpler because no large magnetic fields are required for spin polarization, improvements in accuracy to well below 100 ppm should be feasible.

Although there have been no other measurements of the $2s_{1/2}$-$1s_{1/2}$ $M1$ matrix element in hydrogenic ions, there has been considerable interest in the closely related $1s2s\ ^3S_1$-$1s^2\ ^1S_0$ $M1$ transition rates of heliumlike ions from He to Kr^{34+}.[22] Some of these measurements show indications of nonexponential decay.[23] The present experiment provides an independent check of the relativistic $M1$ transition operator which does not depend on a direct measurement of the radiative decay rate.

The general expression (2.25) for the quenching radiation intensity suggests a number of other experiments that could be performed with hydrogenic ions. For example, if $\hat{k}$, $\hat{E}$, and $\vec{P}$ are all collinear, then the dominant terms are

$$I(\hat{e},\hat{k},\vec{P})=\frac{\alpha k}{4\pi}|V_-|^2[1-(\hat{k}\cdot\hat{e})(\vec{P}\cdot\hat{E})\sin2\beta]\ .$$

If the detector is sensitive only to circularly polarized light ($\beta=\pm\pi$), then the asymmetry with respect to reversal of any one of β, $\hat{k}$, and $\vec{P}$ is $A\simeq|\vec{P}|$. This could provide a direct method for measuring the components of $\vec{P}$. Secondly, as pointed out by Hillery and Mohr,[6] the term $-(\hat{k}\cdot\hat{E})(\vec{P}\cdot\hat{k}\times\hat{E})\ \mathrm{Im}(V^*_-V_+)$ in $\vec{P}\cdot\hat{J}_0$ produces a sizable asymmetry with respect to intensity measurements with polarization-intensitive detectors placed at angles of 45° and 135° to the quenching field. For He^+, the maximum asymmetry is

$$\frac{I(45°)-I(135°)}{I(45°)+I(135°)}=-0.007\,618$$

independent of $\mathscr{E}$ in the limit of weak fields. The effect is roughly proportional to the decay rate of the $2p_{1/2}$ state. An experiment to perform a high-precision measurement of this term is currently in progress.

[1]M. A. Bouchiat and C. Bouchiat, J. Phys. (Paris) 36, 493 (1975); M. A. Bouchiat and L. Pottier, J. Phys. Lett. (Paris) 37, 79 (1976).
[2]S. Chu, E. D. Commins, and R. Conti, Phys. Lett. 60A, 96 (1977).
[3]W. M. Itano, Phys. Rev. A 22, 1558 (1980).
[4]E. U. Condon, Rev. Mod. Phys. 9, 432 (1937).
[5]P. J. Mohr, Phys. Rev. Lett. 40, 854 (1978).
[6]M. Hillery and P. J. Mohr, Phys. Rev. A 21, 24 (1980).
[7]G. W. F. Drake, Phys. Rev. Lett. 40, 1705 (1978).
[8]H. Gould and R. Marrus, Phys. Rev. Lett. 41, 1457 (1978). For reviews of earlier work, see S. J. Brodsky and P. J. Mohr, in *Structure and Collisions of Ions and Atoms,* edited by I. A. Sellin (Springer, Berlin, 1978); H. W. Kugel and D. E. Murnich, Rep. Prog. Phys. 40, 297 (1977).
[9]G. W. F. Drake, S. P. Goldman, and A. van Wijngaarden, Phys. Rev. A 20, 1299 (1979); A. van Wijngaarden and G. W. F. Drake, *ibid.* 17, 1366 (1978).
[10]W. E. Lamb, Jr. and R. C. Retherford, Phys. Rev. 79, 549 (1950); W. E. Lamb, Jr., *ibid.* 85, 259 (1952).
[11]V. Weisskopf and E. Wigner, Z. Phys. 63, 54 (1930).
[12]P. R. Fontana and D. J. Lynch, Phys. Rev. A 2, 347 (1970).
[13]H. K. Holt and I. A. Sellin, Phys. Rev. A 6, 508 (1972).
[14]M. T. Grisaru, H. N. Pendleton, and R. Petrasso, Ann. Phys. (N.Y.) 79, 518 (1973).
[15]G. W. F. Drake and R. B. Grimley, Phys. Rev. A 11, 1614 (1975); G. W. F. Drake, P. S. Farago, and A. van Wijngaarden, *ibid.* 11, 1621 (1975).
[16]E. J. Kelsey and J. Macek, Phys. Rev. A 16, 1322 (1977).
[17]A. I. Akhiezer and V. B. Berestetskii, *Quantum Electrodynamics* (Wiley, New York, 1965), pp. 348–352.
[18]A. R. Edmonds, *Angular Momentum in Quantum Mechanics* (Princeton University Press, Princeton, 1960).
[19]W. R. Ott, W. E. Kauppila, and W. L. Fite, Phys. Rev. A 1, 1089 (1970).
[20]G. W. F. Drake, Phys. Rev. A 3, 908 (1971).
[21]H. W. Kugel, M. Leventhal, and D. E. Murnick, Phys. Rev. A 6, 1306 (1972).
[22]For a review, see J. Sucher, in *Atomic Physics 5,* edited by R. Marrus, M. Prior, and H. Shgart (Plenum, New York, 1977), p. 415.
[23]D. L. Lin and L. Armstrong, Jr., Phys. Rev. A 16, 791 (1977).